Combined Modifications of Mexiletine Pharmacophores for New Lead Blockers of $Na_v1.4$ Channels

Michela De Bellis,[†△] Annamaria De Luca,[†△] Jean F. Desaphy,[†] Roberta Carbonara,[†] Judith A. Heiny,[‡] Ann Kennedy,[‡] Alessia Carocci,[§] Maria M. Cavalluzzi,[§] Giovanni Lentini,[§] Carlo Franchini,[§] and Diana Conte Camerino[†*]

[†]Unit of Pharmacology, Department of Pharmacy-Drug Science, University of Bari, Aldo Moro, Italy; [‡]Department of Molecular and Cellular Physiology, University of Cincinnati and Molecular Research Center, Cincinnati OH; and [§]Unit of Medicinal Chemistry, Department of Pharmacy-Drug Science, University of Bari, Aldo Moro, Italy

ABSTRACT Previously identified potent and/or use-dependent mexiletine (Mex) analogs were used as template for the rational design of new Na_v-channel blockers. The effects of the novel analogs were tested on sodium currents of native myofibers. Data and molecular modeling show that increasing basicity and optimal alkyl chain length enhance use-dependent block. This was demonstrated by replacing the amino group with a more basic guanidine one while maintaining a proper distance between positive charge and aromatic ring (Me13) or with homologs having the chirality center nearby the amino group or the aromatic ring. Accordingly, a phenyl group on the asymmetric center in the homologated alkyl chain (Me12), leads to a further increase of use-dependent behavior versus the phenyl Mex derivative Me4. A fluorine atom in paraposition and one ortho-methyl group on the xylyloxy ring (Me15) increase potency and stereoselectivity versus Me4. Charge delocalization and greater flexibility of Me15 may increase its affinity for Tyr residues influencing steric drug interaction with the primary Phe residue of the binding site. Me12 and Me15 show limited selectivity against Na_v-isoforms, possibly due to the highly conserved binding site on Na_v. To our knowledge, the new compounds are the most potent Mex-like Na_v blockers obtained to date and deserve further investigation.

INTRODUCTION

Voltage-gated sodium channels are therapeutic targets in a large spectrum of membrane hyperexcitability disorders, including cardiac arrhythmias, epilepsies, chronic pain, and myotonias (1,2). In particular, the skeletal muscle sodium channel isoform, $Na_v1.4$ is the molecular target of current first-line therapies against myotonic syndromes. Lidocaine (LA)-like drugs is widely used antimyotonic compounds because they block $Na_v1.4$ in a state- and use-dependent manner. This blocking mechanism relies on the high-affinity drug binding to the channel in its open or inactivated state, and to a slow recovery from inactivation of the drug-bound channel. These actions dampen membrane excitation and prevent reexcitation during membrane repolarization (3,4). However, LA-like compounds can cause undesirable effects and this has led to the discontinuation of mexiletine (Mex) in some countries. Therefore, there is a need for $Na_v1.4$ blocking drugs with greater tissue specificity.

A key factor limiting the further development of $Na_v1.4$-specific blocking compounds is the lack of more complete structure-function information on the interactions of such drugs with the channel. Many previous studies have suggested that hydrophobic blocking drugs have a unique access pathway to the channel pore, unlike the more hydrophilic compounds that access the pore during channel opening. Site-directed mutagenesis studies have identified a cluster of highly conserved residues among the Na_v subtypes that are important for block by LA-like drugs. These residues include DIVS6-Phe-1759 and DIVS6-Tyr-1766, and DIIIS6-Leu-1461 (based on $Na_v1.5$) (5–7). LA-like drugs share a common structural backbone composed of an aromatic ring and a protonable amino group linked by a short alkyl chain. Docking studies of its interaction with $Na_v1.4$ depict a π-cation interaction of the charged amino group with the aromatic ring of Phe-1759 in DIVS6, reinforced by a further dock with nearby Leu-1461 on DIIIS6. The nonpolar tail of LA-like drugs, i.e., the alkyl chains and aromatic ring, participates in hydrophobic interactions with Tyr-1766 in DIVS6.

The structures of several different bacterial voltage-gated sodium channels (Na_vMs) are becoming available. Among these, a newly available crystal structure confirms that corresponding residues align to form a transmembrane cavity for hydrophobic blocking drugs. The channel includes cavities (fenestrations) in the transmembrane region that would allow access of hydrophobic ligands from the membrane to enter the interior of the channel pore. Of importance, these fenestrations are much larger in the open than in the closed state (8,9). The new structural information supports previous findings that voltage-dependent conformational changes of $Na_v1.4$ may favor stronger interactions with these residues and/or better positioning of the drug in the channel pore (3).

Submitted May 25, 2012, and accepted for publication November 21, 2012.

△Michela De Bellis and Annamaria De Luca contributed equally to this work.

*Correspondence: diana.conte@farmbiol.uniba.it

Editor: Michael Pusch.

0006-3495/13/01/0344/11 $2.00

http://dx.doi.org/10.1016/j.bpj.2012.11.3830

Rational, structure-based drug design for sodium channel blockers is limited by such conformational variability and docking energy studies of drug binding interactions for LA-type drugs must necessarily consider the relevant state- and use-dependent Na_v channel conformations. Thus, classical structure-activity relationship studies still provide key information for searching new promising Na_v channel blockers.

In an attempt to find potent use-dependent blockers of $Na_v1.4$ channels, we have previously screened several newly synthesized analogs of the LA-like drugs Mex and tocainide for their inhibitory action on native skeletal muscle sodium currents, providing a foundation for subsequent docking energy studies to identify the molecular determinants of drug action (10,11). We demonstrated that replacement of the methyl group on the asymmetric carbon atom with the lipophilic aromatic phenyl ring (as shown for Me4, Fig.1) increased its potency for blocking resting sodium channels by 10-fold (*tonic block*), but had only a small effect on use-dependent block (UDB) (12,13). A similar increase in potency was observed with the concomitant presence of the phenyl group on the chiral center and a single ortho-methyl group, with or without a chlorine atom in para position, on the xylyloxy ring, suggesting that this pharmacophore is important for proper steric conformation of the drug and its interaction with Na_v (12,14). We also found that lengthening the aminoalkyl chain to increase the distance between the chiral carbon atom and the amino terminal group (as shown for Me2, Fig. 1), decreased its potency in producing tonic block (TB) of resting $Na_v1.4$ and, importantly, produced a corresponding increase in UDB (12–14). Whether this increase is due to the change in physicochemical properties such as pK_a or the simple lengthening of the chain is not yet established (15,16). However, an increase in UDB is pivotal to the therapeutic usefulness of all LA-type compounds in countering abnormal membrane hyperexcitability (17).

This study builds on those findings and uses a panel of newly synthesized LA-type compounds, together with biophysical and molecular analysis of drug-channel interactions, to define the structural requisites for drugs that interact with the LA site on $Na_v1.4$. We searched for novel compounds in which the combination of favorable changes at the main pharmacophores may increase both the potency and use-dependent behavior on skeletal muscle sodium

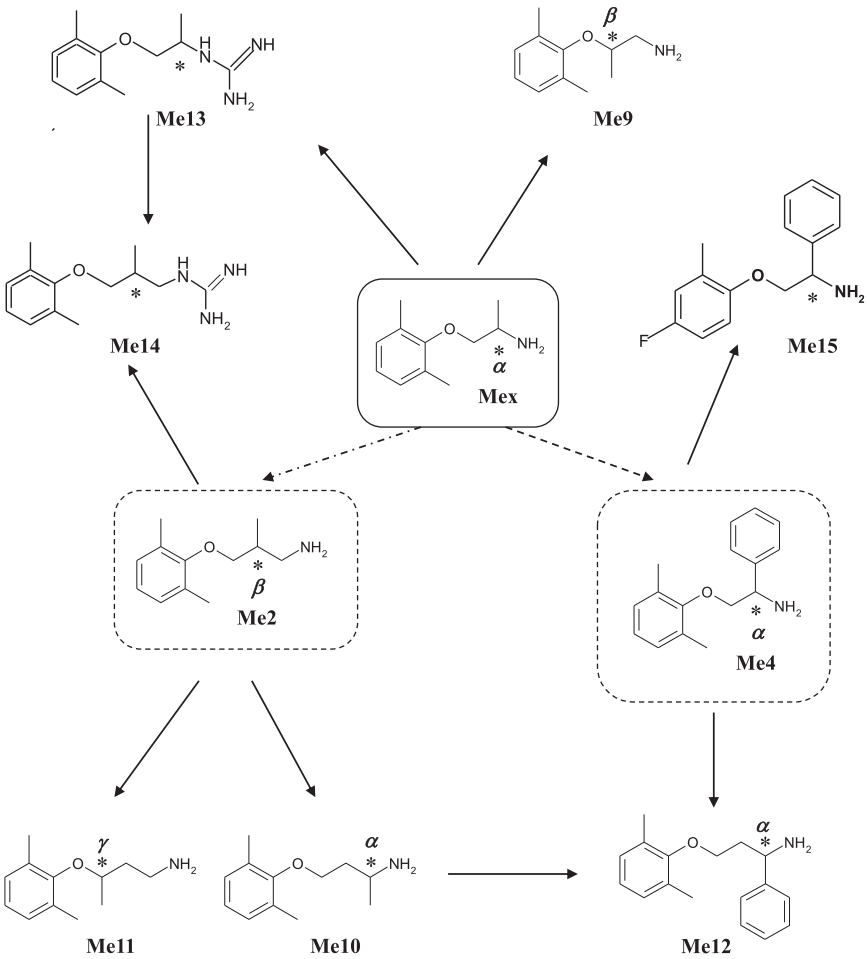

FIGURE 1 Chemical structure of Mex and its newly synthesized analogs. The boxes show the compounds presently tested (*continuous lines*). *Indicates the position of the chiral carbon atom.

channels. The new Mex analogs have modifications to the pharmacophore designed to evaluate:

1. the role of basicity and alkyl chain length in the use-dependent behavior;
2. the role of the position of the stereogenic center of the elongated alkyl chain in use-dependence and stereoselectivity; and
3. the ability of combined modifications to the alkyl chain or the aromatic ring to potentiate use-dependence and stereo selectivity of phenyl derivative.

Biophysical interactions were assessed from measurements of I_{Na} in adult single frog skeletal muscle fibers and the experimental data were interpreted using ab initio molecular modeling. In addition, studies on recombinant human $Na_v1.4$ and $Na_v1.5$ were started to gain insight into the tissue selectivity of the most potent compounds.

MATERIALS AND METHODS

The screening of compounds on I_{Na} of single muscle fibers was carried out by means of voltage-clamp recordings based on methods described by Hille and Campbell (18) and detailed in the paragraph Additional Methods section (in the Supporting Material) (19,20).

Solutions and drugs

The compounds tested are shown in Fig. 1 (21). Chemical names and arbitrary abbreviated nomenclature are provided in the Additional Methods section, along with the composition of solutions with and without drugs.

Pulse protocols and analysis

The TB and UDB exerted by each compound was calculated as the percent reduction of the maximal peak sodium transient ($I_{Na,max}$) elicited by depolarizing steps to −20 mV from the holding potential (HP) of −100 mV at a frequency of 0.3 and 10 Hz, respectively. The use-dependent behavior of test compounds was estimated by the further reduction of I_{Na} that progressively increased above the TB in a frequency-dependent manner until new steady-state amplitude was reached. The degree of UDB was computed as the value of the steady-state $I_{Na,max}$ at this point normalized to the current at the same point in the absence of drug. This parameter reflects the potency of the drug for blocking the channels under conditions of high-frequency stimulation (i.e., as occurs during myotonic action potential firing). The voltage-dependent block was estimated with a pulse protocol of infrequent depolarizing stimulation to −20mV for 10 ms from two different HP values: very negative (−140 mV), and depolarized (−70mV), resembling a pathological condition. As described previously, this protocol reports drug binding to the channel in the inactivated and/or the resting state, respectively (12,13). The concentration-dependence of the drug effect was calculated as the half-maximal blocking concentration (IC_{50}) at −140 mV, which allowed calculation of the affinity constant for the resting state (K_r). The IC_{50} value calculated from a HP of −70mV is influenced both by the higher proportion of channels entering a closed-state inactivation at this potential and by the possible ability of the drug, if acting as an inactivated channel blocker, to modify this distribution in favor of more inactivated channels. The affinity constant of the drug for the inactivated channel (K_i) was computed using its voltage-dependent block, the IC_{50} values, and the relative distribution of channels in the resting or inactivated state obtained from the steady-state inactivation curve (22).

Molecular modeling

Molecular models of protonated *R*-Me1, *R*-Me4, *S*-Me12, and *R*-Me15 were constructed by fragments offered by the SPARTAN PRO (Wavefunction, Irvine, CA) inner fragment library and assuming the suggested default starting geometries. Details of the ab initio molecular modeling are described in the Additional Methods section.

Patch-clamp recordings

Sodium current measurement in HEK293 cells

Transient expression of cardiac channels was achieved by cotransfecting human embryonic kidney (HEK293) cells with 10 μg $hNa_v1.5$ plasmid and 1 μg gene reporter CD8 using the calcium phosphate coprecipitation method. Cells expressing the channel were identified with microbeads coated with anti-CD8 antibody (Dynal, Invitrogen) and used for patch-clamp experiments 24–72 h after transfection. Permanent expression of $hNa_v1.4$ was obtained in HEK293 cells as previously described (23). Sodium currents were recorded at room temperature (21–22°C) by the whole-cell patch-clamp method, using an Axopatch 1D amplifier (Molecular Devices, Sunnyvale, CA) and a 12-bit A-D/D-A interface (Digidata 1440A, Molecular Devices). Voltage-clamp protocols and data acquisition were performed with pClamp software (version 10.2, Molecular Devices). Sodium currents were elicited by 25 ms-long depolarizing test pulses to −30 mV from the holding potential of −120 mV, at two stimulation frequencies: 0.1-Hz to determine TB and 10-Hz to determine UDB. Results were analyzed offline using Clampfit (PClamp package) and SigmaPlot 8.02 (Systat software GmbH, Erkrath, Germany).

Drugs and solutions

Composition of pipette and bath solutions is provided in the Additional Methods section. The compounds *S*-Me12 and *R*-Me15 were solubilized in dimeethyl sulfoxide (DMSO)-supplemented bath solution. The final concentration of DMSO did not exceed 0.2% and had no effects on sodium currents.

Data analysis and statistics

The data were expressed as mean ± SE. IC_{50} values in the various experimental conditions were determined using a nonlinear least squares fit of the concentration-response curves to the following logistic equation: $\text{Effect} = -100/\{1+(K/[\text{drug}])^n\}$, where Effect is the percentage change of I_{Na}; −100 is the maximal percentage block of I_{Na}; K is IC_{50}; n is the logistic slope factor, and [drug] is the molar concentration of the compound (12,14). The $h\infty$ curves were fitted with a single Boltzmann function, and the potential at which 50% of the sodium channels were inactivated ($Vh_{1/2}$) was calculated at the inflection point of the curves (12,19). Statistical significance of differences between couples mean values was estimated using an unpaired Student's *t*-test and considered significant for $p < 0.02$. Statistical significance of differences in IC_{50} values ± SE obtained from the fit was evaluated by a Student's *t*-test, where the number of degrees of freedom is equal to the total number of preparations used to determine each point on the curve minus the number of means determining the curve minus two for the free parameters (13).

RESULTS

Potency of the newly synthesized analogs for tonic and UDB

Role of basicity versus alkyl chain length in the use-dependence

As previously reported (13,14,24), the insertion of a methylene moiety in the alkyl chain of Mex, as in Me2, increases

the use-dependent behavior for blocking I_{Namax} compared to the parent compound (Fig. 1; Table 1), and this is explained by an increased basicity (12–14). Thus, we evaluated whether the change of a highly basic group in place of the amino one of Mex may also increase its use-dependent behavior. To this aim, we synthesized and tested the guanyl derivative of Mex Me13. Guanidine ($NH_2C = NHNH_2$) is a strong base ($pK_a = 13.6$) (25) and the substitution of the nitrogen atoms of guanidine with alkyls, as in the case of Me13, is expected to render it at least as basic as guanidine (26).

Me13 displayed increased potency in tonic and UDB versus Mex, positioning itself in the same rank order of use-dependence as Me2. In fact, Me13 was ~twofold more potent than Mex in tonic and 10-Hz use-dependent block, respectively (Table 1). In agreement with the increased potency of this analog, the concentration-response curves were left-shift compared to Mex for both tonic and 10-Hz use-dependent block, respectively (Fig. S1 *B*). In particular, Me13 showed a high use-dependent behavior, with a ratio (IC_{50} TB/IC_{50} 10-Hz UDB) of 4, which correlates with a strong basicity; in fact, Me13 has a higher pK_a value (12.15 ± 0.70) than Mex (9.28 ± 0.01) (Table S1). However, further elongation of the intermediate alkyl chain by formal insertion of a methylene group in the structure of Me13 to obtain Me14 did not further increase its potency in UDB, despite the stronger basicity of Me14 (Table S1). In fact, the dose-response curves describing the TB by Me14 and Me13 were almost overlapping, whereas that describing the UDB by Me14 at 10-Hz was shifted to the right compared to those of Mex and Me13 (Fig. S1 *B*).

TABLE 1 Concentrations for half-maximal TB and UDB of sodium currents (IC_{50}) by chiral analogs of mexiletine

	Tonic block			Use-dependent block			
Compound	IC_{50} (μM)	*R*	r	10Hz IC_{50} (μM)	*R*	r	TB/UDB
RS-Mex	75 ± 8	*1*	2	23.6 ± 2.8	*1*	1	3
R-Mex	74 ± 82[a]			31 ± 8			2
S-Mex	127.0 ± 2.8			32 ± 7			4
R-Me9	94 ± 8[b]	*1*	1	17.9 ± 1.8	*2*	1	5
S-Me9	104 ± 17			18.7 ± 1.8			6
RS-Me13	53.1 ± 2.7[e,f]	*1*		12.5 ± 1.2[e,f]	*2*		4
R-Me2	175 ± 7	*1*	2	24 ± 8	*2*	1	7
S-Me2	109 ± 4 [a]			17.5 ± 2.1			6
R-Me10	64 ± 6[c]	*1*	1	6.9 ± 0.5[c]	*4*	1	9
S-Me10	78 ± 6			9.2 ± 1.6			8
R-Me11	115 ± 12	*1*	2	19.5 ± 2.8	*4*	2	6
S-Me11	59.1 ± 0.4[a,c]			7.7 ± 1.9[a,c]			8
RS-Me14	46.4 ± 2.7[e]	2		27.8 ± 5.2	1		2
R-Me14	49.9 ± 7.5		1	30.9 ± 8.4		2	2
S-Me14	34.6 ± 3.4[a,c]	2		17.7 ± 2.1[a]	2		2
R-Me4	12.0 ± 0.5	*7*	1	3.4 ± 0.6	*10*	1	4
S-Me4	10.1 ± 0.8			3.1 ± 0.5			3
R-Me12	13.2 ± 0.9	*7*	1	2.9 ± 0.1	*16*	2	4
S-Me12	10.5 ± 0.5[a]			1.9 ± 0.1[a,d]			5
R-Me15	13.6± 0.9[a,d]	*5*	2	1.9 ± 0.2[a,d]	*16*	*6*	7
S-Me15	34.3 ±0.7			10.8 ± 1.6			3

Concentrations able to produce half-maximal response (IC_{50}, μM) in producing a TB and a UDB. The ratio between IC_{50} values during TB and UDB (IC_{50} TB/IC_{50} UDB 10-Hz) is shown to allow an easier comparison of the use-dependent behavior of each compound. The IC_{50} values have been obtained during nonlinear least-square fit of the concentration-response data to the logistic equation described in the Methods. The ratio (*R*) between IC_{50} values of Mex and IC_{50} values of each compound, for the TB and UDB, is also shown to better evaluate the relative potency toward the parent compound. The eudismic ratio (r = IC_{50} distomer/IC_{50} eutomer) is an index of stereoselectivity.

a, b, c, and d show the statistic significance by Student's *t* distribution (for $P < 0.001$ or less) as follows:

[a]between the enantiomers of the same compound;

[b]*R*-Me9 vs. *R*-Mex;

[c]*R*-Me10 and *S*-Me11 vs. *S*-Me2;

[d]*S*-Me12 and *R*-Me15 vs. *S*-Me4;

[e]*RS*-Me13 and *RS*-Me14 vs. *RS*-Mex;

[f]*RS*-Me13 vs. *RS*-Me14.

This finding suggests that Me14 displaces its main pharmacophoric elements (i.e., the aromatic ring and the charged group) in a manner that does not fit the steric requirements of the receptor site on the sodium channel. The guanidinium ion is a highly symmetric, planar Y-delocalized system that presents a distributed cationic charge roughly centered on its iminic carbon atom. Consequently, as can be seen in Fig S2 the distance between the cationic charge and the aromatic ring in Me13 approximates that of Mex homolog Me2, although the two groups are far apart in Me14. This finding supports the idea that the physicochemical properties that are pivotal for use-dependent behavior are secondary to the structural requirements that control drug interaction with the main residues of the receptor site.

Role of the position of the stereogenic center in the optimal alkyl chain length

With respect to the optimal length of the alkyl chain, we evaluated whether the position of its asymmetric center with respect to the main pharmacophore groups may also play a role. The presence of a chiral center near the amino terminal group (Me10) or near the aromatic aryloxy ring (Me11), increased the potency for producing a TB of I_{Na}, compared to Me2. As seen in Fig. S3 *A*, 10 μM of the eutomers *R*-Me10 and *S*-Me11 produced a TB (17 ± 4%, $n = 3$ and 20 ± 5%, $n = 4$, respectively) greater than that observed with the same concentration of *S*-Me2 (6 ± 7%, $n = 4$). Accordingly, the concentration-response curves were left-shifted (Fig. S3 *B*). The relative IC_{50} values of *R*-Me10, *S*-Me11, and *R*-Mex were lower compared to that of *S*-Me2, and the increased potency was not due to an increase in logP (Table S1). Both homologs Me10 and Me11 showed a strong UDB behavior. In fact, the concentration-response curves obtained after a train of depolarizing pulses at 10-Hz were markedly left-shifted compared to those of both Mex and Me2 Fig. S3 *B*. The eutomer *R*-Me10, showed the greatest UDB behavior with a ratio

(IC_{50} TB/IC_{50} 10-Hz UDB) of 9 vs. 6 and 8 for *S*-Me2 and *S*-Me11, respectively (Table 1). Collectively, these results suggest that the higher UDB of these two analogs is explained by their higher estimated pK_a values compared to Me2 and especially to Mex. However, the finding that the higher use-dependence of block by Me10 versus Me11 is not associated with a further increase in pK_a (Table S1) suggests that more specific chemical interactions between Me10 and the receptor site contribute to its potency during frequency-dependent channel transitions. In parallel, the presence of the asymmetric center near the xylyloxy moiety as in Me11 increased its stereoselective interaction versus Me2 and Me10, both during tonic and phasic block, the eudismic ratio (r) being 2 and 3, respectively (Table 1).

To better understand the impact of the chirality center in the alkyl chain on stereoselectivity, we evaluated the effects of Me9, a Mex analog in which the chirality center is nearer to the aromatic xylyloxy ring (Fig. 1). It is noteworthy that this latter change showed almost no stereoselectivity for both TB and UDB, in parallel with a less pronounced use-dependent behavior, compared to its homolog Me2 (Table 1). This finding again suggests that the optimal alkyl chain length must be maintained for allowing combined or individual control of other drug properties.

Effects of combined modifications on alkyl chain or xylyloxy moiety in potent Me4 derivatives

As reported, the replacement of the methyl group on the stereogenic center with the lipophilic aromatic phenyl group, as in Me4, markedly increased its potency for producing TB of I_{Namax} (12,13). The results described in the previous paragraph indicate Me10 as the ideal use-dependent long-chain analog to evaluate the effect of combining the two modifications (Me12, Fig. 1). Interestingly, the combined presence of the phenyl ring and the long chain did not cause any remarkable change in the potency of the drug for TB of I_{Na} compared to *S*-Me4, the IC_{50} value being 10.5 ± 0.5 μM for the eutomer *S*-Me12 (Table 1, Fig. 2 *A*). Accordingly, the concentration-response curves for TB of *S*-Me4 and *S*-Me12 were almost overlapping both being significantly shifted to the left with respect to that *R*-Mex (Fig. 2 *B*). Of importance, *S*-Me12 showed a higher use-dependent behavior than *S*-Me4, the IC_{50} at 10-Hz being ~twofold lower than that of Me4 and up to 16-fold lower than that of Mex (Table 1; Fig. 2 *B*). This high use-dependent behavior is consistent with the increase in basicity expected from lengthening the alkyl chain; in fact Me12 has a higher pK_a value (8.60 ± 0.01) than Me4 (7.89 ± 0.03) (Table S1). Interestingly, Me12 also had a fourfold greater use-dependent behavior compared to its parent compound Me10. This increase is correlated in a more complex manner with physicochemical properties and might be attributable to the ideal logD value plus the pivotal role played by the chain length (Table S1).

In parallel, we investigated the impact on Me4 of structural changes on the xylyloxy ring pharmacophore, based on our previous demonstration that modifications at this level may improve drug potency (14). The introduction of a fluorine atom in the para position of the aromatic ring with the concomitant removal of the one of the two orthol-methyl groups, as in Me15, did not cause any remarkable change in its potency compared to *S*-Me12, despite its relatively modesty basicity. On the other hand, Me15 showed the high stereoselective behavior that was particularly evident during high frequency stimulation. This trend is clearly evident in the left-shift of the concentration response curve of the *R*-enantiomer versus. the *S*-one (Fig. 2 *C*). In particular, the eudismic ratio [IC_{50} distomer/IC_{50} eutomer] was 6 (Table 1), the highest we have ever found with this class of compounds. The latter observation provides compelling evidence for a strong interaction between the aromatic ring, less symmetrically substituted in *R*-Me15 than in *S*-Me12 with its binding site, and that this interaction is able to drive a conformational steric disposition of the other pharmacophore at its site of interaction.

Voltage-dependent block and effects of the Mex derivatives on steady-state inactivation of Na^+ channels

We investigated the channel state-dependent affinity of the various analogs. For each compound, we constructed concentration-response curves for the block produced at two different HP, −140 and −70 mV, in conditions of low-frequency stimulation (Fig. S4). The scale of the potency of the compounds for binding the resting channels (Kr), evaluated at a HP of −140 mV was the same as that found for TB at −100 mV, being Me15≥Me12>Me14>Me13>Me11>Me10 (Table 2). As expected from inactivated channel blockers, an increased potency was observed when the membrane potential was held at −70 mV, at which about half of the sodium channels directly transit from the closed to the inactivated state. In fact, the concentration-response curves of all compounds were clearly shifted to the left with respect to those obtained at −140 mV. The gain of potency for each compound at the more depolarized potential ranged between 2- and 10-fold, with Me12 and Me15 again showing the highest gain of potency. The order of potency was similar to that found for the UDB at 10-Hz. Their affinity for the inactivated state was calculated from the values of K_r and K_{-70}, and confirms the high affinity of *S*-Me12 as an inactivated channel blocker with affinity as low as 1.2 μM (Table 2).

All the test compounds produced a significant and concentration-dependent shift of the h_∞ curves toward

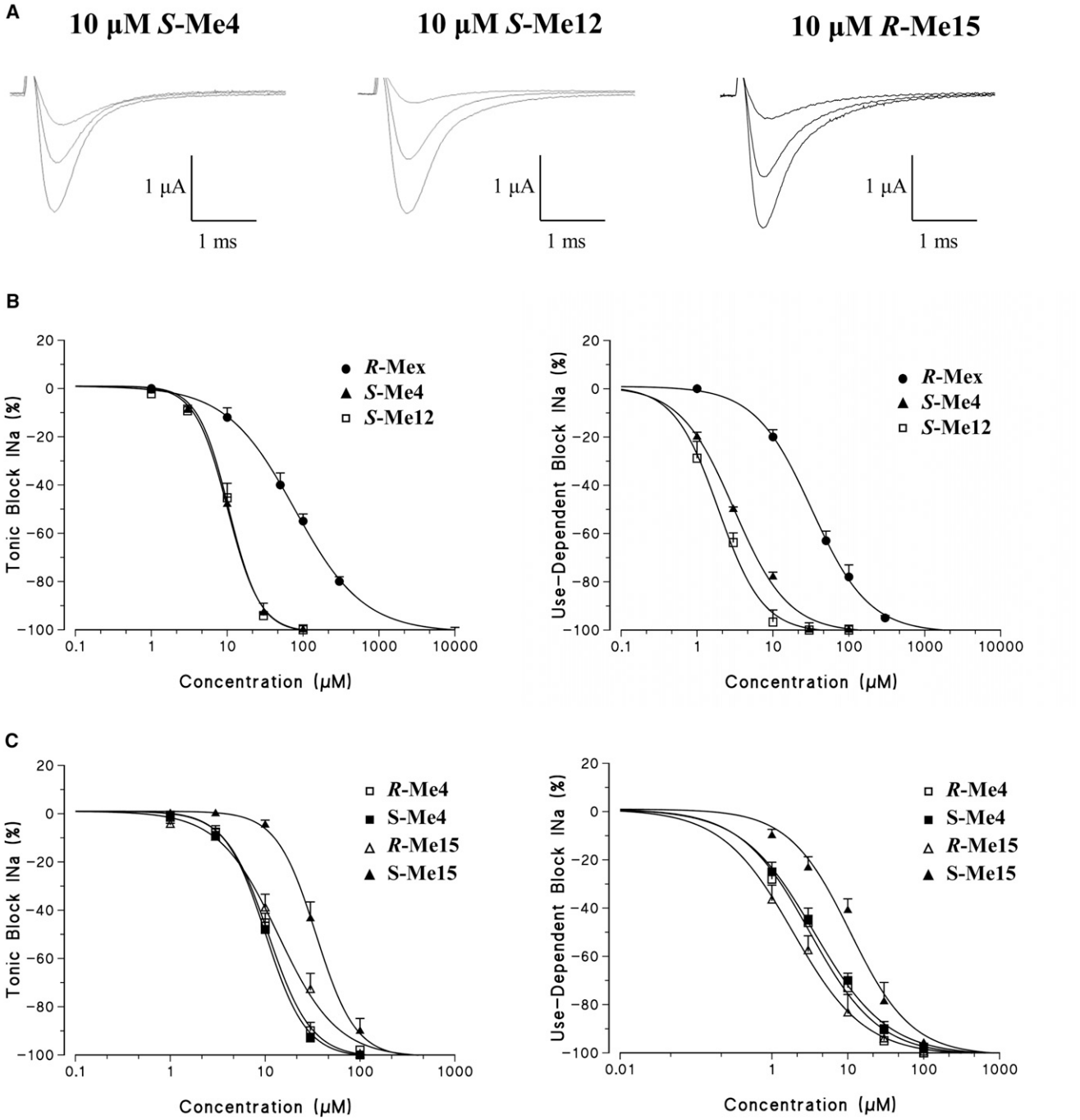

FIGURE 2 Evaluation of the tonic and use-dependent block exerted by analogs *S*-Me4, *S*-Me12, and *R*-Me15. Upper panel *A*: are showing traces of I_{Na} transients recorded in the absence and presence of drug. In each group of traces, the greatest one has been recorded in the absence of drug, with a depolarizing step from the HP of −100 to −20 mV for10 ms. A similar depolarizing stimulus applied after the application of each compound allowed to estimate the TB exerted by the drug (*middle traces*). The smallest current traces correspond to the residual current at the end of the 10-Hz stimulation protocol. The I_{Na} reduction exerted by increasing drug concentrations and evaluated on the first-pulse trace and on the residual steady-state current allowed to construct the dose-response curves for TB and UDB at 10-Hz (*lower* panel *B*). Lower panel *C*: are showing concentration-response curves for TB and 10-Hz UDB of Na^+ currents obtained with enantiomers of Me4 and Me15. The curves fitting the experimental points were obtained using the logistic function described in Materials and Methods. Each value is the mean ± SE from 4 to 8 fibers of the percent block of I_{Na} observed in the presence of each concentration of drugs versus I_{Na} in the absence of the drug in the same fiber.

more negative potentials, with a potency related to their ability to block peak I_{Na}. Among the homologs, the isomer *S*-Me12, which was the most potent in blocking sodium channels, was also the most effective in shifting the h_∞ curves toward more negative potentials (Fig. S5).

TABLE 2 Voltage-dependent block of sodium currents by chiral analogs of Mex

	Voltage-dependent block		Inactivated state block
	HP −140 mV	HP −70 mV	
Drug	IC_{50} (μM); K_r	IC_{50} (μM); K_{-70}	Calculated K_i (μM)
R-Me10	117 ± 4	14.2 ± 1.2	11.8
S-Me11	82 ± 12	6.8 ± 1.2	5.5
S-Me12	13.1 ± 0.4	1.3 ± 0.1	1.2
RS-Me13	68 ± 3	31.7 ± 0.4	28.6
RS-Me14	56 ± 7.	21.5 ± 0.4	18.8
R-Me15	12.8 ± 1.7	1.2 ± 0.3	1.9

Abbreviations: HP, holding potentials; IC_{50}, half-maximal blocking concentration; K_i, affinity constant for the inactivated state; K_r, affinity constant for the resting state.

The columns from left to right are as follows: drug used; IC_{50} values at two different HP values: −140 and −70mV; inactivated-state block refers to the affinity constants for inactivated sodium channels (K_i) according to the equation in Materials and Methods.

Ab initio molecular modeling of Me12 or Me15 vs. Me4

Why does S-Me12 have the same activity as its inferior homologs R- and S-Me4?

The longer alkyl chain of Me12 versus Me4 increased its use-dependent behavior but did not alter its potency in exerting a TB. To further understand the molecular bases for this difference, we undertook an ab initio molecular modeling study of *S*-Me12—the eutomer of Me12—and *R*-Me4. These enantiomers were chosen based on the lack of stereoselectivity of Me4 during UDB and the observation that, despite its stereochemical descriptor, *S*-Me12 shares the same configuration as *R*-Me4. The HF/6-31G**//HF/3-21G* most stable conformers of these compounds are shown in Fig. S6. Despite homologation, both compounds place their main pharmacophoric elements—the protonated amino group and the xylyloxy ring—at the same distance (5.18 ± 0.07 Å, measured from the charged nitrogen atom to the phenyl ring centroid). It is likely that an intramolecular hydrogen bond contributes to conformer stabilization, this interaction being tighter for *S*-Me12 than *R*-Me4 as reflected by the distance between H and O atoms—the donated and accepting atoms in the hydrogen bonds (1.61 Å and 1.83 Å, respectively) (Fig. S6). In line with this observation, the most positive electrostatic potential located near the protonated nitrogen atom was lower for *S*-Me12 than for *R*-Me4 (154.7 Kcal/mol and 164.4 Kcal/mol, respectively) (Fig. S6), reflecting higher delocalization of the positive charge through hydrogen bonding for *S*-Me12. Interestingly, the number of HF/6-31G**//HF/3-21G* stable conformations falling in the window of 5 Kcal/mol over the global minimum conformer was lower for *S*-Me12 than *R*-Me4 (2 and 4, respectively), although the superior homolog has one more rotatable bond. This observation may reflect a higher constraint for *S*-Me12 than *R*-Me4, possibly explaining the higher eudismic ratio found for the superior homolog of this pair of enantiomers.

Why do changes at the xylyloxy ring in Me15 lead to high potency and stereoselectivity vs. Me4?

The ab initio molecular modeling study on *R*-Me15 showed the presence of two almost degenerate conformers as the most stable ones at the HF/6-31G**//HF/3-21G* level (Fig. 3, *A* and *B*): in conformer **a** (absolute minimum conformer) the plane containing the aryloxy ring and the one made by the ether functional group are almost orthogonal (synclinal, dihedral angle: –81); whereas, in conformer **b** (less stable for only 0.3 Kcal/mol) the two planes are synperiplanar (dihedral angle: –25°). Thus, rotation around the Car-O bond is less hindered in *R*-Me15 than in *R*-Me4, which presents only an orthogonal disposition of these planes for all conformers within the window of 5 Kcal/mol over the global minimum. The electrostatic potential map for the most stable HF/6-31G**//HF/3-21G* conformer of *R*-Me15 (Fig. 3 *C*) demonstrates that, due to the strong electron withdrawing effect of the fluorine atom, the electronic distribution on the aromatic ring is quite different from the one observed in *R*-Me4, with most of the electron negative charge concentrating on the halogen atom. Taken together, the observed reduction of both electron density of the aromatic ring and steric hindrance around the CAr-O bond should favor delocalization of the oxygen lone pairs and polarizability of the aromatic moiety. Interestingly, by performing the same molecular modeling study on the chlorine isologue *R*-Me1 (14), a synperiplanar conformer was found only at 1.8 Kcal/mol over the global minimum conformer (data not shown). This finding supports a role of the electron withdrawing effect of the fluorine atom in determining the ring plane orientation.

The results of this modeling analysis predict the experimental data well. In fact, despite its relatively modest basicity, *R*-Me15 was as potent as *S*-Me12 and also had the highest eudismic ratio in the series. The latter observation supports the involvement of a strong interaction between the aromatic rings, less symmetrically substituted in *R*-Me15 than in *S*-Me12, with its binding site. The high stereoselectivity observed does support the role of the aryloxy moiety as a pharmacophoric element able to condition the interaction of the main pharmacophoric group—the protonated amine—with its binding site. In particular, the fluorine atom, which is highly electron dense in the Me15 molecule, in addition to contributing to the disposition of the CAr-O bond, may confer stronger electronic effects, hydrogen bonds, and halogen bonds than the xylyloxy rings without alogens or with a chlorine substituent.

Muscle versus cardiac effect of most potent derivatives

Based on these results, we undertook an initial investigation of the specificity of the two most potent derivatives, *S*-Me12

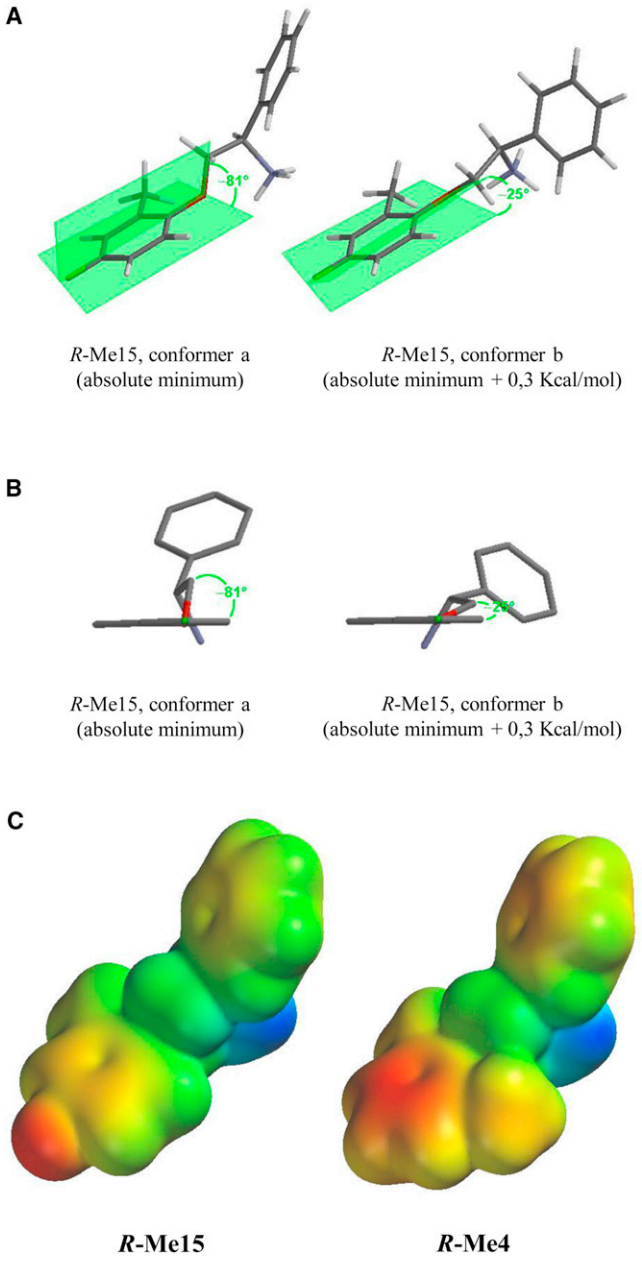

FIGURE 3 (*A*) The two most stable conformers of Me15—**a**, synclinal, and **b**, synperiplanar; dihedral angles between the aromatic ring and ether functional group containing planes are highlighted. (*B*) Newman projections obtained observing **a** and **b** from the fluorine atom side in the direction of the bond connecting the latter to the aryloxy ring (for the sake of simplicity hydrogen atoms have been omitted). (*C*) Electrostatic potential maps for *R*-Me15 and *R*-Me4.

and *R*-Me15, for skeletal compared to cardiac muscle sodium channels. The two compounds were tested at a single concentration of 10 μM, close to the half-maximal one, on $hNa_v1.4$ and $hNa_v1.5$ channels expressed permanently or transiently, respectively, in HEK293 cells. I_{Na} was recorded in the whole-cell patch-clamp configuration. Both TB and UDB were estimated under conditions of low (0.1-Hz) and high (10-Hz) frequency of stimulation from the holding potential of −120 mV to −30 mV. Fig. S7 shows representative traces of sodium currents recorded before (CTRL) and after application of drug (10 μM). Both compounds were ~10-fold more potent than Mex in producing TB of $hNa_v1.4$ and $hNa_v1.5$; their TB at 10 μM was comparable or greater than that observed with 100 μM Mex (27,28). As seen in Fig.S7, *S*-Me12 was more effective in blocking $hNa_v1.5$ than $hNa_v1.4$ at low stimulation frequencies, with a calculated specificity ratio (block $Na_v1.5$/block $Na_v1.4$) of 2.6-fold. A similar result was found for *R*-Me15 (ratio 4). However, consistent with results on native myofibers, *S*-Me12 exhibited a high use-dependence on $hNa_v1.4$. In particular, *S*-Me12 had a twofold greater use-dependence on $hNa_v1.4$ compared to $hNa_v1.5$, becoming equipotent on both channel types (ratio = 1), whereas *R*-Me15 was less use dependent. Therefore, the newly synthesized compounds, although more potent than Mex in absolute terms, did not show any specific advantage in channel subtype specificity. Their apparent greater affinity for heart over skeletal muscle compared to Mex can be explained by both compounds being high-affinity inactivated channel blockers in combination with the different biophysical profile of the channel isoforms. In fact, the inactivated state is more favored for heart compared to skeletal muscle channel subtypes.

DISCUSSION

Understanding the complex molecular interactions that underlie UDB of Na_v channels by drugs is important for a more complete understanding of Na_v structure-function relationships as well as for the rational design of therapeutic compounds for treating membrane disorders of hyperexcitability. The voltage-gated sodium channels represent an important therapeutic target for the development of drugs useful in the treatment of many diseases in which the channel may be directly or indirectly involved (1,29). Current private research in the pharmaceutical industry is mainly focused on identifying sodium channel blockers that may have therapeutic application in widespread pathological conditions such as neuropathic pain (30,31). There is much less research on the development of blockers that target Na_v subtypes relevant to the more rare human disorders such as myotonic syndromes and periodic paralyses (1). In parallel, various academic groups are involved in site-directed mutagenesis and molecular biology combined with biophysical studies aimed at further understanding the molecular mechanisms that underlie drug-receptor interactions and the molecular determinants for tissue selectivity (3,8,32). Only limited published information is available on the structural determinants for potent and use-dependent modulation of voltage-gated sodium channels, also because the structures of the most potent compounds are undisclosed or patent-covered before reaching the market.

In this context, our laboratory has been committed for many years to characterizing the molecular determinants of LA-like drugs; the rational design of new sodium channel blockers that can be safely used to treat excitability disturbances in patients affected by the drug-orphan skeletal muscle channelopathies (1). Our studies have provided key information about structural requirements and then a concrete contribution to facilitate, in a larger context, the development of new molecules of potential clinical interest.

Our previous studies showed that the activity of Mex-like sodium channel blockers is strongly modulated by the part of the molecule near the asymmetric carbon atom. In fact, the presence of a lipophilic moiety such as a phenyl group on the chiral center enhances its potency up to 10-fold (12,13). Lengthening the alkyl chain in association with increased basicity increases the use-dependent behavior (12–14). These structural modifications improved the antimyotonic activity, evaluated in vitro and in vivo as the ability to counteract myotonic symptoms in the myotonic adr/adr mouse (20,33). On the basis of these findings, and with the dual aim of improving the therapeutic profile and gaining more insight in structural determinants for drug action, we further investigated the role of basicity in the use-dependent behavior. It is well accepted that most of the use-dependency derives from the quota of charged molecules reaching the local-anesthetic binding site (1). It has been recently shown that the experimentally derived pK_a value of Mex is 9.28 (21); therefore, Mex is expected to be 99% ionized at physiological pH. In principle, further increasing its basicity should not enhance its use-dependence. However, charged species experience a lower dielectric environment in the channel pore than in bulk solution and this reduces their effective pK_a once in the membrane interior (34). In other words, when interacting with its target, Mex behaves as a weaker base than what may be anticipated on the basis of its experimentally derived pK_a (35). Consequently, Mex analogs designed to be more basic than the reference compound might display a more favorable blocking activity profile. In agreement with this view, we have shown that the presence of a guanidinum group (Me13) increases both its pK_a and use-dependent behavior. This compound shows a profile similar to the elongated chain homolog Me2, which also has a higher pK_a than Mex. On the other hand, further elongation of the alkyl chain of Me13, as done in Me14, did not further potentiate its UDB, despite the stronger basicity of Me14. These observations are in agreement with previous reports showing the importance of both basicity and optimal alkyl chain length per se for sodium channel blocking compounds (13,21,24,36,37). As shown in Fig. S2, the distance between the cationic charge and the aromatic ring in Me13 is greater than that in Mex while approximating that for Mex homologs (e.g., Me2,) and being shorter than that of the less effective Me14. These results underscore the importance of an optimal alkyl chain length and a basic pK_a for use-dependent behavior. These observations support the importance of a basic pK_a for a use-dependent behavior as secondary requirements versus structural backbone that controls drug interaction with main residues. In this respect, the asymmetric center can also play a pivotal role. Me10 and Me11, in which the chirality center in the elongated alkyl chain is adjacent to the main pharmacophore groups (i.e., the amino terminal group or the aromatic xylyloxy ring, respectively) were approximately twice as potent in determining TB as Me2. This behavior can be explained by a greater flexibility of the alkyl chain due to the noncentral position of the asymmetric center, thereby ensuring an optimal conformation for interaction with the binding site, as suggested by Sheldon et al. (1991) (36). This view is also supported by the hypothesis of vertical orientation of the drug in the open channel (3). Accordingly, the longer alkyl chain in Me10 increases its use-dependence and can again be explained by a general higher basicity that enhances its interaction with the binding site. The gain of potency of Me10 in high-frequency stimulation conditions supports its potential interest as a lead compound for controlling hyperexcitability disorders such as myotonia. Me10 may also have pharmacokinetic advantages in that its structure is expected to be less liable to metabolic oxidative deamination in vivo than Me11 (21).

These considerations led us to test whether the combination of the homologated alkyl chain with the phenyl moiety on the asymmetric center (Me12) may enhance the use-dependent interaction of LA-type drugs with Na_v channel. This combination of structural requirements did not significantly change the potency for TB of I_{Na} but significantly enhanced UDB (e.g., when the phenyl derivative and short alkyl chain were combined in Me4). Although the increase in pK_a can again account for the increased use-dependence, molecular modeling helped us to gain insight in the similar potency of Me12 vs. Me4. Despite homologation, both compounds place their main pharmacophoric elements—the protonated amino group and the aryloxy ring—at the same distance, whereas an intramolecular hydrogen bond contributes to tighter conformer stabilization for Me12 than Me4.

An important remaining question is whether it is possible to further enhance the potency of LA-like compounds on the $Na_v1.4$ channel by the use of enantiomers. Pure enantiomers may be clinically useful due to enantioselective metabolism and the possible presence in vivo of active stereoselective metabolites (38,39). Although residues potentially involved in a stereoselective three point interaction of LA-type drugs with the sodium channel have been described, stereoselectivity of sodium channel blockers in various tissues is rather modest (40). A limited stereoselective block of sodium channels also occurs in skeletal muscle (12,15). However, the structural requirements for stereoselectivity in blocking channels are not fully known. Interestingly, in this work, we observed that the compound in which the asymmetric center

is nearby to the xylyloxy ring (Me11) and one in which an o-methyl was removed and a fluorine atom was introduced in the 4-position of the aromatic ring (Me15) showed the highest degree of stereoselectivity. It is likely that, in Me11, the methyl substituent tunes the orientation of the xylyloxy ring and constrains it by steric hindrance through intramolecular bonding. Accordingly, previous studies using tocainide analogs in which the chiral center is constrained into a rigid proline cycle are those showing the greatest stereoseletive behavior to date (15).

The greater stereoselectivity of Me15 may have a more complex explanation, because the main structural changes are present at the level of the xylyloxy ring, rather far from the chirality center.

It is generally accepted that the aromatic ring of Mex and analogs interacts with the Na_v channel at IVS6-Tyr (5,10). However, elegant site-directed mutagenesis studies by Ahern et al. (2) demonstrated that the interaction of LA and its quaternary ammonium derivative QX-130 with IVS6-Tyr is not an aromatic-aromatic one, supporting previous observations by Courtney and Strichartz (35). The latter authors suggested that the ring acts more as an aliphatic than an aromatic group, due to the ability of the o-methyl groups to force the carboxamide group to a direction perpendicular to the plane of the aromatic ring, thereby producing a resonance decoupling effect. On the basis of the previous results, Fozzard et al. (4) have recently concluded that an aliphatic interaction of the aromatic moiety of local anesthetics with IVS6-Tyr plays a secondary role in the drug-receptor interaction. Their study reinforces the view that the main electrostatic interaction of the charged amino group is with IVS6-Phe and that IVS6-Tyr plays only a secondary role. However, our recent results obtained with a series of Mex analogs require the role of the xylyloxy in the interaction with the binding site to be reconsidered (28). In particular, the introduction of hydroxyl groups onto the xylyloxy moiety of mexiletine modifies the high-affinity binding of the protonated amine terminal to IVS6-Phe through a cooperativity between the two pharmacophore groups, and mutation of IVS6-Tyr further impairs such cooperativity (28). These observations are consistent with the previous finding, obtained using a series of phenyl analogs of Mex, that the introduction of a chlorine atom in the 4-position of the xylyloxy ring along with the replacement of an o-methyl group increases drug potency and inverts stereoselectivity. This finding first suggested a possible relationship between the site of interaction of the protonated amino group on the stereogenic center and the aromatic moiety interaction site (12). Thus, we speculated that Mex analogs may have further interactions with the IVS6-Tyr binding site beside the merely aliphatic one. The current results obtained with enantiomers of Me15 in which an o-methyl was removed and a fluorine atom was introduced in the 4-position of the aromatic ring, favor these putative interactions. Such interactions are further supported by molecular modeling. The disruption of symmetry at the xylyloxy ring reduces steric hindrance, thus allowing resonance between the lone pairs of the oxygen atom and the aromatic sextet. In addition, the introduction of a fluorine atom in the para position reduces the electron density of the aromatic ring thus making it complimentary to the supposed electron rich ring of IVS6-Tyr. Furthermore, the electron dense fluorine atom may confer additional hydrogen and/or halogen bonding interactions (41). Accordingly, the analysis of conformers confirmed that the rotation around the C_{Ar}-O bond is less hindered in *R*-Me15 than in *R*-Me4, the latter presenting only an orthogonal disposition compared to a higher number of more planar conformers of Me15. Together, these considerations suggest the occurrence of a strong interaction of the less symmetrically substituted aromatic ring of *R*-Me15, with its Tyr binding site which is able to influence the interaction of the main pharmacophore group—the protonated amine—with its binding site at the Phe residue. Our current results provide new, to our knowledge, insights into the relative role of pharmacophores for binding to crucial residues on Na_v and suggest novel lead molecules for enhancing potency, use-dependence, and stereo selective behavior. The new compounds may be helpful in future docking studies and energetic modeling, especially in relation to IVS6-Tyr binding.

Finally, our initial tests of the activity of the most potent derivatives on recombinant human sodium channels confirm the poor tissue selectivity of this class of compounds against different Na_v channel isoforms. Their modest differences in potency against cardiac and skeletal muscle Na_v channels is most likely due to differences in state-dependent binding, with the cardiac $hNa_v1.5$ channel having more resting inactivation than the skeletal muscle $hNa_v1.4$ channel. Future studies will be devoted to testing the most promising analogs on other Na_v isoforms, such as the CNS, to gain further insight into their pharmacological profile. Nevertheless, because use-dependence properties selectively address the activity of a compound against pathological conditions, the new compounds Me10, Me12, and Me15 deserve further investigation of their potency against membrane hyperexcitability both in vitro and in vivo.

Policy and ethics

The work described has been carried out in accordance with EC Directive 86/609/EEC for animal experiments.

SUPPORTING MATERIAL

Seven figures, one table, additional methods, and reference (42) are available at http://www.biophysj.org/biophysj/supplemental/S0006-3495(12)05077-1 .

This work has been supported by Telethon-Italy, Project GGP10101. The contribution of Association-Française contre les Myopathies (AFM), Project MYOTONIADRUGS, is also acknowledged.

REFERENCES

1. Camerino, D. C., J. F. Desaphy, …, A. Liantonio. 2008. Therapeutic approaches to ion channel diseases. *Adv. Genet.* 64:81–145.
2. Ahern, C. A., A. L. Eastwood, …, R. Horn. 2008. New insights into the therapeutic inhibition of voltage-gated sodium channels. *Channels (Austin).* 2:1–3.
3. Sheets, M. F., H. A. Fozzard, …, D. A. Hanck. 2010. Sodium channel molecular conformations and antiarrhythmic drug affinity. *Trends Cardiovasc. Med.* 20:16–21.
4. Fozzard, H. A., M. F. Sheets, and D. A. Hanck. 2011. The sodium channel as a target for local anesthetic drugs. *Front Pharmacol.* 2:68.
5. Ragsdale, D. S., J. C. McPhee, …, W. A. Catterall. 1994. Molecular determinants of state-dependent block of Na^+ channels by local anesthetics. *Science.* 265:1724–1728.
6. Li, H. L., A. Galue, …, D. S. Ragsdale. 1999. A molecular basis for the different local anesthetic affinities of resting versus open and inactivated states of the sodium channel. *Mol. Pharmacol.* 55:134–141.
7. Nau, C., S. Y. Wang, and G. K. Wang. 2003. Point mutations at L1280 in $Na_v1.4$ channel D3-S6 modulate binding affinity and stereoselectivity of bupivacaine enantiomers. *Mol. Pharmacol.* 63:1398–1406.
8. Payandeh, J., T. Scheuer, …, W. A. Catterall. 2011. The crystal structure of a voltage-gated sodium channel. *Nature.* 475:353–358.
9. McCusker, E. C., C. Bagnéris, …, B. A. Wallace. 2012. Structure of a bacterial voltage-gated sodium channel pore reveals mechanisms of opening and closing. *Nat Commun.* 3:1102.
10. Lipkind, G. M., and H. A. Fozzard. 2005. Molecular modeling of local anesthetic drug binding by voltage-gated sodium channels. *Mol. Pharmacol.* 68:1611–1622.
11. Carrieri, A., M. Muraglia, …, C. Pacifico. 2009. 2D- and 3D-QSAR of tocainide and mexiletine analogues acting as $Na_{(v)}1.4$ channel blockers. *Eur. J. Med. Chem.* 44:1477–1485.
12. De Luca, A., F. Natuzzi, …, D. C. Camerino. 2000. Molecular determinants of mexiletine structure for potent and use-dependent block of skeletal muscle sodium channels. *Mol. Pharmacol.* 57:268–277.
13. De Luca, A., S. Talon, …, D. Conte-Camerino. 2003. Inhibition of skeletal muscle sodium currents by mexiletine analogues: specific hydrophobic interactions rather than lipophilia per se account for drug therapeutic profile. *Naunyn Schmiedebergs Arch. Pharmacol.* 367:318–327.
14. De Luca, A., F. Natuzzi, …, D. C. Camerino. 1997a. Inhibition of frog skeletal muscle sodium channels by newly synthesized chiral derivatives of mexiletine and tocainide. *Naunyn Schmiedebergs Arch. Pharmacol.* 356:777–787.
15. Talon, S., A. De Luca, …, D. Conte Camerino. 2001. Increased rigidity of the chiral centre of tocainide favours stereoselectivity and use-dependent block of skeletal muscle $Na(^+)$ channels enhancing the anti-myotonic activity in vivo. *Br. J. Pharmacol.* 134:1523–1531.
16. De Luca, A., M. De Bellis, …, D. C. Camerino. 2012. Searching for novel anti-myotonic agents: pharmacophore requirement for use-dependent block of skeletal muscle sodium channels by N-benzylated cyclic derivatives of tocainide. *Neuromuscul. Disord.* 22:56–65.
17. Jurkat-Rott, K., and F. Lehmann-Horn. 2010. State of the art in hereditary muscle channelopathies. *Acta Myol.* 29:343–350.
18. Hille, B., and D. T. Campbell. 1976. An improved vaseline gap voltage clamp for skeletal muscle fibers. *J. Gen. Physiol.* 67:265–293.
19. De Luca, A., F. Natuzzi, …, D. Conte Camerino. 1995. Stereoselective effects of mexiletine enantiomers on sodium currents and excitability characteristics of adult skeletal muscle fibers. *Naunyn Schmiedebergs Arch. Pharmacol.* 352:653–661.
20. De Luca, A., S. Pierno, …, D. C. Camerino. 1997b. Evaluation of the antimyotonic activity of mexiletine and some new analogs on sodium currents of single muscle fibers and on the abnormal excitability of the myotonic ADR mouse. *J. Pharmacol. Exp. Ther.* 282:93–100.
21. Carocci, A., A. Catalano, …, D. Conte Camerino. 2010. Synthesis and in vitro sodium channel blocking activity evaluation of novel homochiral mexiletine analogs. *Chirality.* 22:299–307.
22. Bean, B. P., C. J. Cohen, and R. W. Tsien. 1983. Lidocaine block of cardiac sodium channels. *J. Gen. Physiol.* 81:613–642.
23. Desaphy, J. F., A. Dipalma, …, D. C. Camerino. 2009. Involvement of voltage-gated sodium channels blockade in the analgesic effects of orphenadrine. *Pain.* 142:225–235.
24. Duranti, A., C. Franchini, …, D. Conte Camerino. 2000. Homologation of mexiletine alkyl chain and stereoselective blockade of skeletal muscle sodium channels. *Eur. J. Med. Chem.* 35:147–156.
25. Angyal, S. J., and W. K. Warburton. 1951. The basic strengths of methylated guanidines. *J. Chem. Soc.* 2492–2494.
26. Raczyńska, E. D., M. K. Cyrański, …, K. Duczmal. 2003. Consequences of proton transfer in guanidine. *J. Phys. Org. Chem.* 16:91–106.
27. Catalano, A., J. F. Desaphy, …, C. Franchini. 2012. Synthesis and toxicopharmacological evaluation of m-hydroxymexiletine, the first metabolite of mexiletine more potent than the parent compound on voltage-gated sodium channels. *J. Med. Chem.* 55:1418–1422.
28. Desaphy, J. F., A. Dipalma, …, D. Conte Camerino. 2012. Molecular insights into the local anesthetic receptor within voltage-gated sodium channels using hydroxylated analogs of mexiletine. *Front.Pharmacol.* 3:1–12.
29. Ghelardini, C., J. F. Desaphy, …, D. C. Camerino. 2010. Effects of a new potent analog of tocainide on hNav1.7 sodium channels and in vivo neuropathic pain models. *Neuroscience.* 169:863–873.
30. Theile, J. W., and T. R. Cummins. 2011. Recent developments regarding voltage-gated sodium channel blockers for the treatment of inherited and acquired neuropathic pain syndromes. *Front Pharmacol.* 2:1–14.
31. Zuliani, V., M. Rivara, …, G. Costantino. 2010. Sodium channel blockers for neuropathic pain. *Expert Opin. Ther. Pat.* 20:755–779.
32. Catterall, W. A. 2000. From ionic currents to molecular mechanisms: the structure and function of voltage-gated sodium channels. *Neuron.* 26:13–25.
33. De Luca, A., S. Pierno, …, D. C. Camerino. 2004. New potent mexiletine and tocainide analogues evaluated in vivo and in vitro as antimyotonic agents on the myotonic ADR mouse. *Neuromuscul. Disord.* 14:405–416.
34. Westman, J., Y. Boulanger, …, I. C. Smith. 1982. Charge and pH dependent drug binding to model membranes. A 2H-NMR and light absorption study. *Biochim. Biophys. Acta.* 685:315–328.
35. Courtney, K. R., and G. R. Strichartz. 1987. Structural elements which determine local anesthetic activity. *In* Local Anesthetics, Handbook of Experimental Pharmacology, *Vol. 81*. G. R. Strichartz, editor. Springer Verlag, New York. 67.
36. Sheldon, R. S., R. J. Hill, …, L. M. Wilson. 1991. Aminoalkyl structural requirements for interaction of lidocaine with the class I antiarrhythmic drug receptor on rat cardiac myocytes. *Mol. Pharmacol.* 39:609–614.
37. Tenthorey, P. A., R. L. DiRubio, …, P. D. McMaster. 1979. New antiarrhythmic agents. 3. Primary beta-amino anilides. *J. Med. Chem.* 22:1182–1186.
38. De Bellis, M., A. De Luca, …, D. Conte Camerino. 2006. Evaluation of the pharmacological activity of the major mexiletine metabolites on skeletal muscle sodium currents. *Br. J. Pharmacol.* 149:300–310.
39. Catalano, A., A. Carocci, …, D. Conte Camerino. 2004. Stereospecific synthesis of "para-hydroxymexiletine" and sodium channel blocking activity evaluation. *Chirality.* 16:72–78.
40. Nau, C., S. Y. Wang, …, G. K. Wang. 1999. Point mutations at N434 in D1-S6 of mu1 $Na(^+)$ channels modulate binding affinity and stereoselectivity of local anesthetic enantiomers. *Mol. Pharmacol.* 56:404–413.
41. Zhou, P., F. Tian, …, Z. Shang. 2010. Rediscovery of halogen bonds in protein-ligand complexes. *Mini Rev. Med. Chem.* 10:309–314.
42. Fu, Y., A. Struyk, …, S. Cannon. 2011. Gating behaviour of sodium currents in adult mouse muscle recorded with an improved two-electrode voltage clamp. *J. Physiol.* 589:525–546.